Desalination and Water Treatment
www.deswater.com

doi:10.5004/dwt.2017.21372

88 (2017) 41–51
September

Analytical characteristic equation of N identical evacuated tubular collectors integrated single slope solar still

D.B. Singh[a,*], V.K. Dwivedi[b], G.N. Tiwari[c], Navneet Kumar[b]

[a]*Centre for Energy Studies, Indian Institute of Technology Delhi, HausKhas, New Delhi, 110016, India, email: dbsiit76@gmail.com*
[b]*Galgotias College of Engineering and Technology, Greater Noida, 201306, India, email: vkdwivedi94@gmail.com (V.K. Dwivedi), navneet_mech48@yahoo.com (N. Kumar)*
[c]*Bag Energy Research Society (BERS), Sodha BERS Complex, Plot No. 51, Mahamana Nagar, Karaudi, Varanasi (UP), 22 10 05, India, email: gntiwari@ces.iitd.ernet.in*

Received 26 February 2017; Accepted 26 August 2017

ABSTRACT

In this paper, analytical expression for characteristic equation of single slope solar still included with series connected N identical evacuated tubular collectors (N-ETC-SS) has been developed. The derivation is based on fundamental energy balance equations for various components of the proposed system. The analytical result of the proposed N-ETC-SS has been compared with results reported by earlier researchers for the same basin area under similar climatic condition. The analysis has been done for a typical day in the month of June for climatic condition of New Delhi at 0.14 m water depth under optimized condition. It has been concluded that daily energy efficiency is higher by 22.65% and 55.63% for N-ETC-SS than N identical partially covered photovoltaic thermal (PVT) compound parabolic concentrator collectors integrated single slope solar still and conventional single slope solar still respectively. Moreover, daily yield, exergy, energy and exergy efficiency have been computed.

Keywords: N-ETC-SS; Characteristic equation; Energy; Exergy; Efficiency

1. Introduction

The solar desalination of water with the help of the proposed active solar distillation system can be one of the best alternatives to assuage the contemporary issue of the scarcity of potable water in far flung areas. In the proposed active solar still, the external heat is added to the basin using evacuated tubular collectors (ETC). Rai and Tiwari [1] investigated active solar still in forced mode theoretically for the first time and concluded that the daily yield of active solar still was higher by 24% than conventional solar still. In unison, Zaki et al. [2] studied the active solar still under natural circulation mode for the first time and concluded that the maximum enhancement in distillate output was 33% higher in comparison to conventional solar still. Solar still can be integrated with a number of series connected FPC to form a closed loop so that hot water can be discharged either directly or indirectly by providing heat exchanger in the basin. Single slope solar still (SS) included with inverted absorber asymmetric line-axis CPC collector was investigated by Yadav and Yadav [3] and they concluded that the production of potable water was improved as compared to conventional solar still because solar energy was provided to solar still both from top and bottom concurrently ensuing in enhanced temperature difference between water surface and glass cover. An experimental investigation of solar still having mirrors at interior walls and coupled with FPC was done by Badran and Tahaineh [4]. They observed an enhancement in distillate output by 36% as compared to conventional solar still. It happened due to enhanced temperature difference between water surface and inner surface of glass cover. Abdel Rehim and Lasheen [5] studied basin type SS by integrating solar parabolic trough collector and heat exchanger. Serpentine Oil was used as working fluid in collector. The amount of distillate output obtained from such system was 18% higher as compared to conventional solar still because of the attainment of higher water temperature in basin as water received solar energy from top and also through heat exchanger in basin. Tripathi and

*Corresponding author.

Tiwari [6] explored experimentally basin type SS included with two collectors and operating in forced mode. They concluded that higher production of potable water was obtained during off-sunshine hours due to heat storage effect at higher depth. Badran et al. [7] explored basin type solar still (double slope) which was included with FPC and operating in forced mode. They concluded that the production of potable water was higher by 52% as compared to conventional solar still. Taghvaei et al. [8] studied experimentally SS coupled with FPC to assess the long term performance (continuous 10 days) and recommended a higher depth of water for practical application as the amount of potable water production and efficiency were found to be higher at higher depth due to heat storage effect.

El-Sebaii et al. [9] compared the performance of single basin active solar still theoretically between with and without a sensible storage material (sand) and reported that daily productivity of the solar still with storage was 23.8% higher than that when it was used without storage. An experimental study regarding the performance of various designs of active solar still was done by Arslan under closed cycle mode and he obtained highest overall daily efficiency for the circular box active solar still design [10]. In a variation, a slowly rotating light-weight hollow drum was partially submerged in solar still cavity and an improvement of 20–30% in the production of potable water was reported as compared to conventional solar still [11]. However, the production of potable water becomes 60% higher than the conventional solar still if the basin of an FPC integrated solar still is partitioned [12]. A considerable enhancement in productivity is also obtained if thermal energy is supplied to solar still by circulating heat transfer fluid at its bottom. It was reported that doubling the heat transfer fluid rate effected a 9% enhancement in the production of potable water. The relation between production of potable water and the heat transfer fluid rate is thus non-linear [13]. A novel tri-generation system employing PVT collectors was designed by Calise et al. [14] for seawater desalination in European Mediterranean countries, known to have abundant renewable sources but deprived of fossil fuels and water resources. Ibrahim et al. [15] investigated experimentally the performance of modified solar still consisting of external air cooled condenser and reported an enhancement of 16.2% and 29.7% in the production of potable water and thermal efficiency respectively for the proposed system over conventional solar still.

Active solar distillation system can be made self sustainable so that it can operate even in remote areas having abundant sunlight but electrical power is not available and the system can generate electrical energy too if need arises. It can be done by including a photovoltaic (PV) panel with FPC coupled to the basin of solar still. The integration of PV panel to collector was proposed by Kern and Russell [16] and it was reported that electrical efficiency was enhanced if fluid was allowed to pass below the panel. A theoretical study of such system was done by Hendrie [17]. In continuation of this approach, an experimental study of SS by incorporating two series connected FPCs (one partially covered with PV) was done by Kumar and Tiwari [18–22] and an enhancement in production of potable water by more than 3.5 times over conventional solar distillation system was reported. They developed empirical relation for heat transfer coefficient and also reported that the payback period of active solar distillation system lied in the range of 3.9–23.9 years. It was extended for double slope active solar still by Singh et al. [23]. Further, Tiwari et al. [24] and Singh et al. [25] extended their work by partially covering both series connected identical FPCs with PV panels. They performed experimental investigation and reported that though the exergy efficiency and overall thermal efficiency values of the system where both the FPCs are partially covered with PV panels are better, the thermal efficiency is lower than the system reported by Kumar and Tiwari [21] and Singh et al. [23]. Also, value of annual productivity varies from 120.29% to 883.55% indicating that the proposed system was feasible. The optimum number of collectors on the basis of exergy efficiency was found to be 4 for 50 kg water mass in the basin of active solar still coupled with a number of PVT-FPCs as reported by Gaur and Tiwari [26].

Eltawil and Omara [27] studied a solar distillation system consisting of SS, FPC, spraying unit, perforated tubes, solar air collector and PV panel to improve the production of potable water and supply electrical power. They reported an enhancement in the production of potable water by 51–148% over conventional solar still depending on the type of modification. Saeedi et al. [28] performed optimization of PVT solar still on the basis of energy efficiency using simulation technique and reported optimum mass flow rate and number of collectors as 0.044 kg/s and 7 respectively. Singh and Tiwari [29–31] performed theoretical study on basin type solar stills included with N identical PVT-CPC collectors for New Delhi climatic condition and reported that the performance of double slope was better than the similar single slope set up at 0.14 m water depth under optimized condition due to higher energy, exergy and lower embodied energy for double slope set up. They also reported that the performance of single slope was better than double slope PVT-CPC active solar still on the basis of average daily productivity, thermal and overall thermal efficiencies if depth of water in the basin is higher than 0.31 m and vice versa. Singh et al. [32] investigated the performance of SS augmented with evacuated tubes in natural mode in which one end of all tubes were inserted into the basin and concluded that overall energy and exergy efficiencies has lied in the range of 5.1–54.4% and 0.15–8.25% respectively during the sunshine hours at 0.03 m water depth for a typical day in the month of summer. Further, Kumar et al. [33] investigated SS augmented with evacuated tubes in forced mode in which one end of all tubes were inserted into the basin and concluded that the daily yield was 3.47 kg at 0.01 m water depth and 0.006 kg/s mass flow rate of for climatic condition of New Delhi.

The contemporary literature survey implies that the analytic expression for characteristic equation of single slope solar still included with N identical series connected evacuated tubular collectors (N-ETC-SS) has not been reported by any researchers. Recently, Mishra et al. [34] have reported the development of characteristic equation for N identical ETC connected in series. These collectors have not been analyzed by incorporating with single slope solar still. To accomplish this research gap, this paper presents the derivation of expression for characteristic equation of N-ETC-SS. In the proposed system, N identical ETC form a closed loop with single slope solar still as outlet of Nth

ETC is discharged to the basin and 1st ETC is fed with water from basin with the help of pump. The proposed system is different from the system of earlier researcher in two ways. Firstly, a number (N) of identical FPC/CPC have been replaced by N identical ETC. Secondly, a number (N) of ETC have been connected in series instead of inserting one end of all collectors to the basin as reported by Singh et al. [32] and Kumar et al. [33]. A comparison of analytical results of the proposed N-ETC-SS with similar set up reported by earlier researchers has also been carried out. The main aim of the proposed investigation can be stated as follows.

(i) To develop analytical expression for characteristic equation of N-ETC-SS based on the inscription of basic energy balance equations for various components of the system.
(ii) To compute daily production of potable water (yield), energy and exergy of the proposed system for a typical day in the month of June for New Delhi climatic condition.
(iii) To compute daily energy and exergy efficiencies of the proposed system.
(iv) To compare the proposed N-ETC-SS with N-PVT-CPC-SS (N identical partially covered photovoltaic thermal (PVT) compound parabolic concentrator collectors integrated single slope solar still) [29], and CSS (conventional single slope solar still) [35] for the same basin area under similar climatic condition on the basis of daily production of potable water, energy, exergy, energy efficiency and exergy efficiency.

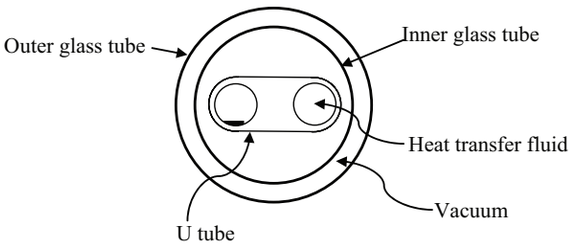

Fig. 1. Cross sectional view of evacuated tubular collector (ETC).

2. System description

Fig. 1 shows the cross sectional view of evacuated tubular collector (ETC), Fig. 2 shows the schematic diagram of the proposed N-ETC-SS and Table 1 represents the exhaustive specification of the system. There are N numbers of identical ETC in the proposed system. Each ETC consists of an inner copper tube through which water is allowed to flow and outer evacuated coaxial glass tube. The inner surface of evacuated coaxial glass tube is coated. The evacuated coaxial glass tube consists of two tubes and an evacuated space is provided between two glass tubes to minimize the heat loss by convection. The radius of inner copper tube is 0.0125 m. The inner radius of inner glass tube of evacuated coaxial glass tube is 0.0165 m. The outer radius of outer glass tube of evacuated coaxial glass tube is 0.024 m. The thickness of inner/outer glass tube of evacuated coaxial glass tube is 0.002 m. The inner copper tube is covered by copper plate to facilitate the transfer of heat to water flowing through the inner copper tube. The outlet of first ETC is connected to the inlet of second ETC; the outlet of second ETC is connected to the inlet of third ETC and so on. This type of arrangement of collectors is called series connection and it has been taken because our aim is to increase the temperature of water in the basin to get higher distillate. The hot water available at the outlet of Nth ETC is discharged to basin and inlet of 1st ETC is fed with water from basin with the help of pump resulting in the formation of closed loop. An inclination of 30° has been provided to all series connected ETC in the

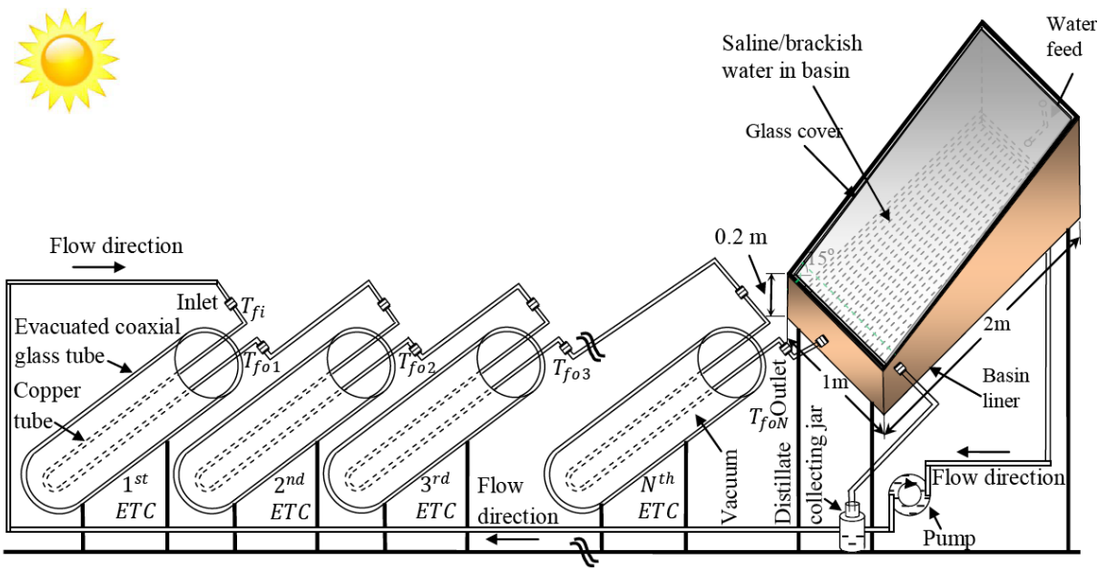

Fig. 2. Schematic diagram of the proposed single slope solar still incorporated with N identical ETC connected in series (N-ETC-SS).

Table 1
Specifications of single slope solar still incorporated with N identical ETC single slope active solar still

Component	Specification	Component	Specification
Single slope active solar still			
Length	2 m	Cover material	Glass
Width	1 m	Orientation	South
Inclination of glass cover	15°	Thickness of glass cover	0.004 m
Height of smaller side	0.2 m	K_g	0.816 W/m-K
Material of body	GRP	Thickness of insulation	0.1 m
Material of stand	GI	K_i	0.166 W/m-K
Evacuated tubular collector (ETC)			
Type and no. of collectors	ETC , N		0.8 $(\alpha)_p$
DC motor rating	12 *V*, 24 *W*		0.968 F
Radius of inner copper tube	0.0125 m		0.95 $(\tau)_g$
Thickness of copper tube	0.0005 m		1.09 K_g (Kg/m-k)
Outer radius of outer glass tube of evacuated coaxial glass tube	0.024 m	Angle of ETC with horizontal	30°
Inner radius of inner glass tube of evacuated coaxial glass tube	0.0165 m	Length of each copper tube	2.0 m
Thickness of outer/inner glass tube of of evacuated coaxial glass tube	0.002 m		

proposed system with an aim to obtain yearly maximum solar radiation. DC motor pump can be run either by grid supply or photovoltaic module. The function of pump is to overcome the pressure drop so that water circulates through water collectors and basin of solar still. Water while passing through pipes of water collector receives heat and gets heated and this heated water is discharged to the basin.

The single slope active solar still has an effective basin area of 2 m × 1 m and it is made up of glass reinforced plastic (GRP). It is oriented toward south to get maximum annual solar intensity. A transparent glass inclined at an angle of 15° with the horizontal has been taken as condensing cover of the solar still. It is sealed with the help of window-putty. The inner surfaces of bottom and side walls of solar still are painted black so that maximum portion of solar flux is absorbed.

The solar flux at the outer surface of transparent glass is transmitted to water after reflection and absorption. Water mass reflects and absorbs some portion of transmitted solar flux and transmits the remaining part to basin liner. Basin liner absorbs almost total radiation falling on its surface. Hence, temperature of basin liner increases which transmits heat to water and temperature of water rises. Water gets evaporated due to temperature difference between the surface of water and glass cover. This evaporated water gets condensed at the inner surface of glass cover through film type condensation. The condensed water trickles down to the channel fixed to the front side of solar still and it is collected in an external container (jar) through pipe. Saline/brackish water flows to the basin with the help of pipe through an opening provided at the rear wall of solar still. An opening is also given at the bottom to facilitate the washing of basin after some use. The entire unit is fixed on iron stand.

3. Thermal modeling

Following assumptions reported by Singh and Tiwari [29–31], characteristic equations of the proposed N-ETC-SS have been developed which are as follows.

3.1. Useful energy gain for N identical ETC connected in series

Following Mishra et al. [35], the rate of useful thermal output from N identical ETC connected in series can be written as,

$$\dot{Q}_{uN} = \frac{\left(1-K_k^{\,N}\right)}{\left(1-K_k\right)}\left(AF_R(\alpha\tau)\right)_1 I(t) + \frac{\left(1-K_k^{\,N}\right)}{\left(1-K_k\right)}\left(AF_R U_L\right)_1 \left(T_{fi} - T_a\right) \tag{1}$$

where, $\left(AF_R(\alpha\tau)\right)_1 = PF_1(\alpha\tau^2)A_R F_R$; $\left(AF_R U_L\right)_1 = \left(1-K_k\right)\dot{m}_f c_f$; $PF_1 = \frac{h_{pf}}{F' h_{pf} + U_{tpa}}$;

$U_L = \frac{U_{t,pa}.h_{pf}}{F' h_{pf} + U_{t,pa}}$; $F_R = \frac{\dot{m}_f C_f}{U_L A_R}\left[1 - \exp\left(-\frac{2\pi r' L' U_L}{\dot{m}_f c_f}\right)\right]$; $K_K = \left(1 - \frac{A_R F_R U_L}{\dot{m}_f c_f}\right)$

$h_{pf} = 100 W m^2 K^{-1}$ and $U_{t,pa} = \left[\frac{Ro_2}{R_{o1} h_i} + \frac{R_{o2}\ln\left(\frac{Ri_2}{Ri_1}\right)}{K_g} + \frac{1}{C_{ev}} + \frac{R_{o2}\ln\left(\frac{Ro_2}{Ro_1}\right)}{K_g} + \frac{1}{h_o}\right]^{-1}$

In the set-up reported by Mishra et al. [35], a number (N) of series connected ETC do not form loop. However, they form a loop with basin of single slope solar still in the proposed system as hot water available at the outlet of Nth ETC is discharged to basin and 1st ETC is fed with water from basin with the help of pump. Hence, the value of T_{fi} is

same as the value of T_w The expression of temperature at the exit of Nth ETC (T_{foN}) can written as

$$T_{foN} = \frac{(AF_R(\alpha\tau))_1}{\dot{m}_f C_f}\frac{\left(1-K_k^{\ N}\right)}{\left(1-K_k\right)}I(t) + \frac{(AF_R U_L)_1}{\dot{m}_f C_f}\frac{\left(1-K_k^{\ N}\right)}{\left(1-K_k\right)}T_a + K_k^{\ N}T_{fi} \quad (2)$$

where, the value of T_{fi} is equal to T_w The hot water obtained at the exit of Nth ETC is discharged to the basin. Hence, the value of T_{wo} is equal to the value of T_{foN}.

3.2. Energy balance equations for single slope solar still

Equations resulting from balancing of energy for various components of active single slope solar still can be inscribed as follows.

Inner surface of glass cover

$$\alpha_g' I_S(t)A_g + h_{1w}\left(T_w - T_{gi}\right)A_b = \frac{K_g}{L_g}\left(T_{gi} - T_{go}\right)A_g \quad (3)$$

Here, $\alpha_g' = \left(1-R_g\right)\alpha_g$ represents the fraction of solar flux absorbed by the glass cover and $h_{1w} = h_{rwg} + h_{cwg} + h_{ewg}$ represents the rate of total heat transfer coefficient from water surface to inner surface of glass cover.

Outer surface of glass cover:

$$\frac{K_g}{L_g}\left(T_{gi} - T_{go}\right)A_g = h_{1g}\left(T_{go} - T_a\right)A_g \quad (4)$$

where $h_{1g} = h_{rg} + h_{cg}$ *or* $h_{1g} = 5.7 + 3.8V$

Water mass in basin:

$$\dot{Q}_{uN} + \alpha_w' I_S(t)A_b + h_{bw}\left(T_b - T_w\right)A_b = h_{1w}\left(T_w - T_{gi}\right)A_b + M_w C_w\frac{dT_w}{dt} \quad (5)$$

where $\alpha_w' = \left(1-R_g\right)\left(1-\alpha_g\right)\left(1-R_w\right)\alpha_w$ which is the fraction of solar flux absorbed by water mass and $\dot{Q}_{uN}$ is the rate of useful thermal output from N identical hybrid PVT collectors connected in series.

Basin liner:

$$\alpha_b' I_s(t)A_b = h_{bw}\left(T_b - T_w\right)A_b + h_{ba}\left(T_b - T_a\right)\mathrm{A_b} \quad (6)$$

where $\alpha_b' = \left(1-R_g\right)\left(1-\alpha_g\right)\left(1-R_w\right)\left(1-\alpha_w\right)\alpha_b$ which represents the fraction of solar flux absorbed by basin liner.

The expression of various unknown terms used in Eqs. (3)–(6) are given in Appendix-A. Using Eq. (1) and Eqs. (3)–(6), one can get the first order differential equation of water temperature (T_w) for N-ETC-SS as follows.

$$\frac{dT_w}{dt} + a_1 T_w = f_1(t) \quad (7)$$

The expression for a_1 and $f_1(t)$ used in Eq. (7) are given in Appendix-A. The solution of differential Eq. (7) can be inscribed as

$$T_w = \frac{\bar{f}_1(t)}{a_1}\left(1-e^{-a_1 t}\right) + T_{w0}e^{-a_1 t} \quad (8)$$

where T_{w0} is the temperature of water at $t = 0$ and $\bar{f}_1(t)$ is the average value of $f_1(t)$ during the time interval 0 to t. After computing the value of T_w with the help of Eq. (8), one can evaluate values of glass temperature (T_{gi} and T_{go}) using Eqs. (3) and (4) as follows.

$$T_{gi} = \frac{\alpha_g' I_s(t)A_g + h_{1w}T_w A_b + U_{c,ga}T_a A_g}{U_{c,ga}A_g + h_{1w}A_b} \quad (9)$$

$$T_{go} = \frac{\frac{K_g}{L_g}T_{gi} + h_{1g}T_a}{\frac{K_g}{L_g} + h_{1g}} \quad (10)$$

After computing the value of water temperature (T_w) and glass temperature, the hourly production of potable water ($\dot{m}_{ew}$) can be computed as follows.

$$\dot{m}_{ew} = \frac{h_{ewg}A_b\left(T_w - T_{gi}\right)}{L} \times 3600 \quad (11)$$

where L stands for the amount of thermal energy required to evaporate unit mass of water (latent heat) and can be computed with the help of the expression for the same reported by Fernandez and Chargoy [36] and Toyama [37].

Following Nag [38], hourly and daily exergy gain of the proposed system can be inscribed as

$$\dot{G}_{ex} = h_{ewg}A_b\left[\left(T_w - T_{gi}\right) - \left(T_a + 273\right)\ln\left\{\frac{\left(T_w + 273\right)}{\left(T_{gi} + 273\right)}\right\}\right] \quad (12)$$

$$G_{ex} = \sum_{t=24}^{t=1}\left[h_{ewg}A_b\left[\left(T_w - T_{gi}\right) - \left(T_a + 273\right)\ln\left\{\frac{\left(T_w + 273\right)}{\left(T_{gi} + 273\right)}\right\}\right]\right] \quad (13)$$

The hourly and daily overall exergy gain for N-PVT-CPC-SS and CSS have been computed using expressions reported by Singh and Tiwari [29], Singh et al. [34] respectively.

Following Tiwari [39], hourly and daily energy gain of the proposed system can be inscribed as

$$\dot{E} = \frac{\left(\dot{\mathrm{m}}_{\mathrm{ew}} \times \mathrm{L}\right)}{3600} \quad (14)$$

$$E = \frac{\sum_{t=1}^{t=24}\left[\dot{m}_{ew} \times L\right]}{3600} \quad (15)$$

The hourly and daily overall energy gain for N-PVT-CPC-SS and CSS have been computed using expressions reported by Singh and Tiwari [29] and Singh et al. [34] respectively.

The hourly and daily exergy efficiency for the proposed system can be inscribed as

$$\eta_{hourly,ex} = \frac{\dot{G}_{ex}}{\dot{E}x_c(t) + \left[0.933 \times A_b \times I_S(t)\right] + P_u} \times 100 \quad (16)$$

$$\eta_{daily,ex} = \frac{G_{ex}}{\sum_{t=1}^{10}\left[\dot{E}x_c(t) + \left[0.933 \times A_b \times I_S(t)\right] + P_u\right]} \times 100 \quad (17)$$

where $\dot{E}x_c(t) = \left(\dot{m}_f \times C_t\right)\left[\left(T_{foN} - T_{fi}\right) - (T_a + 273) \times \ln\frac{(T_{foN} + 273)}{(T_{fi} + 273)}\right]$ (18)

The hourly and daily exergy efficiency for N-PVT-CPC-SS and CSS have been computed using expressions reported by Singh and Tiwari [30] and Singh et al. [34] respectively.

The hourly and daily energy efficiency for the proposed system can be inscribed as

$$\eta_{hourly,en} = \frac{\dot{E}}{\left[\dot{Q}_{uN}(t) + A_b I_s(t) + \frac{P_u}{0.38}\right]} \times 100 \quad (19)$$

$$\eta_{daily,en} = \frac{E}{\sum_{t=1}^{24}\left[\dot{Q}_{uN}(t) + A_b I_s(t) + \frac{P_u}{0.38}\right] \times 3600} \times 100 \quad (20)$$

The hourly and daily exergy efficiency for N-PVT-CPC-SS and CSS have been computed using expressions reported by Singh and Tiwari [30] and Singh et al. [34] respectively.

4. Methodology

The following methodology has been adopted for the numerical calculation of the proposed system and its comparison with results of similar systems proposed by earlier researchers.

Step I

Solar flux on the horizontal surface and ambient air temperature for a typical day in the month of June has been taken from Indian Metrological Department (IMD), Pune, India. The value of solar flux on the inclined surface at 30° north latitude has been computed using Liu and Jordan formula with the help of MATLAB. The hourly variation of global and beam radiation on horizontal surface and ambient air temperature have been presented in Fig. 2.

Step II

Eq. (2) has been used to compute the numerical value of T_{foN}. Basin water and glass temperatures of N-ETC-SS have been calculated using Eqs. (8)–(10). Values of various heat transfer coefficients have been computed using expressions given in Appendix-A. Then, the production of potable water for N-ETC-SS has been calculated using Eq. (11).

Step III

The hourly and daily exergies have been computed using Eqs. (12) and (13) respectively. Similarly, the hourly and daily energies have been computed using Eqs. (14) and (15) respectively.

Step IV

The hourly and daily exergy efficiencies have been computed using Eqs. (16) and (17) respectively. Similarly, hourly and daily energy efficiencies have been computed using Eqs. (19) and (20) respectively.

Step V

Results obtained from the proposed N-ETC-SS have been compared with results of N-PVT-CPC-SS and CSS.

5. Results and discussion

All associated equations and climatic data viz. hourly solar intensity, ambient air temperature and average wind velocity have been supplied to computational program using MATLAB. The hourly solar intensity on horizontal surface and atmospheric air temperature for a typical day in the month of June for New Delhi climatic condition are given in Fig. 3. The average wind velocity for the month of June is 4.11 m/s. The output obtained from the computational program is shown in Figs. 7–14.

Fig. 4 represents the variation of maximum temperature of fluid at the outlet of Nth ETC ($T_{foN,max}$) with number of collector (N) for a given mass flow rate of collector fluid ($\dot{m}_f$) of N-ETC-SS for a typical day in the month of June. The addition of heat per unit time $\dot{Q}$ in the basin of N-ETC-SS is given by $\dot{Q} = \dot{m}_f C_f\left(\Delta T_f\right)$ where $\Delta T_f = T_{foN} - T_{fi}$ It means that the value of $\dot{Q}$ is directly proportional to $\dot{m}_f$. So, we should have higher value of $\dot{m}_f$. However, increase in the value of $\dot{m}_f$ results in lowering the value of T_{foN} because liquid in pipes of collector will get lesser time for heat absorption. Also, the amount of heat loss from absorber increases with the increase in the value of $\dot{m}_f$. Hence, one will have to compromise between the value of $\dot{m}_f$ and T_{foN}.

It is observed from Fig. 4 that curves are getting closer to each other as value of $\dot{m}_f$ increases and they start almost overlapping beyond $\dot{m}_f$ = 0.016 kg/s because collector fluid gets lesser and lesser time to gain heat in pipes of collector and the rate of heat transfer from absorber plate to water increases with the increase in value of $\dot{m}_f$. It means that the value of $T_{foN,max}$ becomes almost constant beyond $\dot{m}_f$ = 0.016

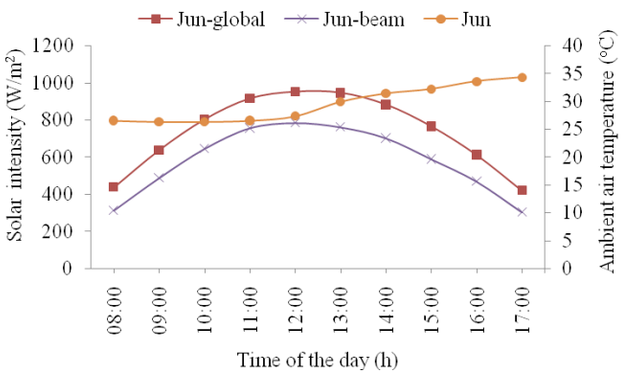

Fig. 3. Hourly variation of radiation on horizontal surface and ambient air temperature for a typical day in the month of June.

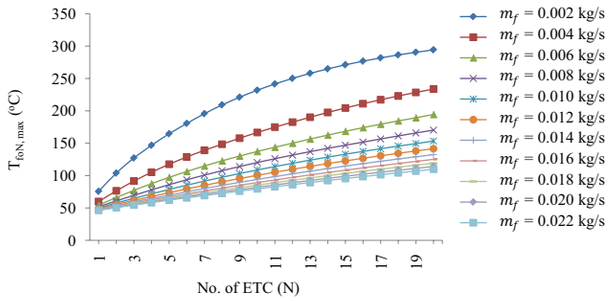

Fig. 4. Variation of $T_{foN,max}$ with N for given $\dot{m}_f$ of collector fluid of N-ETC-SS for a typical day in the month of June.

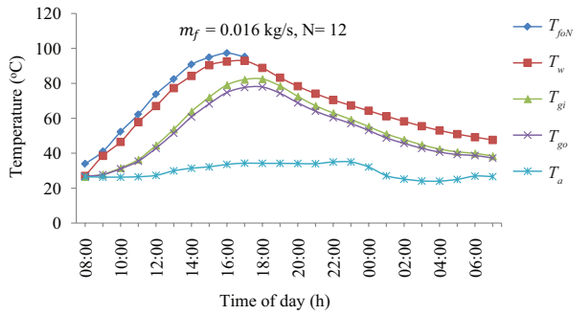

Fig. 5. Hourly variation of various temperatures of N-ETC-SS for a typical day in the month of June.

kg/s. Hence, optimum value of $\dot{m}_f$ can be taken as 0.016 kg/s. Further, value of $T_{foN,max}$ increase as N is increased at optimum value of mass flow rate and number of collectors. However, the value of $T_{foN,max}$ becomes more than 100°C beyond N = 12. Hence, optimum value of N can be taken as 12 since the working fluid in ETC is water. The thermal modeling will cease to be valid if the value of $T_{foN,max}$ becomes greater than 100°C. To tackle the case of higher temperature (>100°C), another fluid can be used by inserting heat exchanger in the basin to transfer the thermal energy to basin water and avoid the mixing of collector fluid with basin water.

Fig. 5 represents hourly variation of various temperatures of proposed N-ETC-SS at 0.14 m water depth, optimum values of N and for a typical day in the month of June. It is observed that the maximum value of difference in water temperature and glass temperature occurs at 13:00 because maximum value of solar intensity occurs at 12:00 noon. Also, glass temperatures are lower than basin water temperature which is as per expectation as it should occur for getting the water evaporated at accelerated rate. Basin water temperature is lesser than T_{foN} because outlet of Nth ETC is fed to basin and mixing of collector fluid (water) and basin water occurs.

Fig. 6 represents hourly variation of various heat transfer coefficients (HTC) and production of potable water of N-ETC-SS for a typical day in the month of June. It is observed that the maximum value of hourly production of potable water occurs at 15:00 because the production of potable water is the function of both evaporative heat transfer coefficient and ΔT. Here, ΔT stands for the difference between water temperature and glass temperature. It is also observed that values of convective and radiative HTC are lower which are as per expectation because they are responsible for losses.

Fig. 7 represents hourly variation of daily production of potable water with mass flow rate forN-ETC-SS for a typical day in the month of June. The value of daily production of potable water has been found to decrease with the increase in the value of $\dot{m}_f$ because value of T_{foN} decreases as collector fluid gets lesser and lesser time to gain heat in pipes of collector and the rate of heat transfer from absorber plate to water increases with the increase in value of $\dot{m}_f$. It results in lowering the value of T_w and hence lowering the value of ΔT. Fig. 8 represents the variation of daily yield with N at 0.016 kg/s mass flow rate for N-ETC-SS for a typical day in the month of June. It is observed that the daily yield/production of potable water increases with the increase in

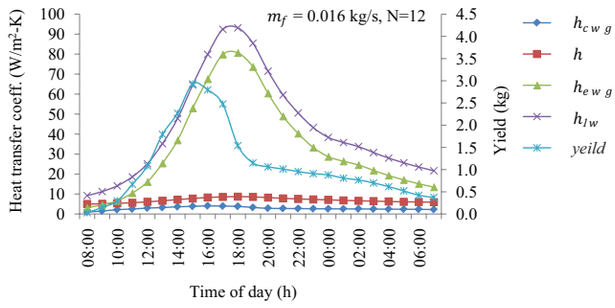

Fig. 6. Hourly variation of heat transfer coefficient and yield of N-ETC-SS for a typical day in the month of June.

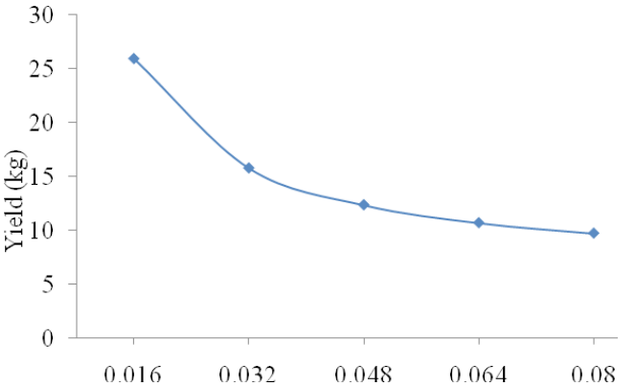

Fig. 7. Hourly variation of daily yield of N-ETC-SS for a typical day in the month of June.

value of N because the amount of thermal energy added to basin water increase with the increase in number of collectors. However, we cannot have $N > 12$ because the temperature of water becomes more than 100°C for the same.

Fig. 9 represents the variation of the production of potable water with types of system at 0.14 m water depth under optimized condition. It is observed that the value of production of potable water is higher by 70.95% for N-ETC-SS than CSS. However, the production of potable water is lower by 6.04% for N-ETC-SS than N-PVT-CPC-SS. The production of potable water for N-ETC-SS is higher than CSS because

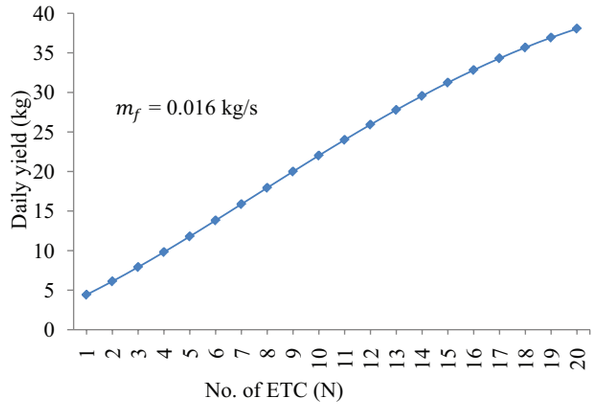

Fig 8. Variation of daily yield with N for N-ETC-SS for a typical day in the month of June.

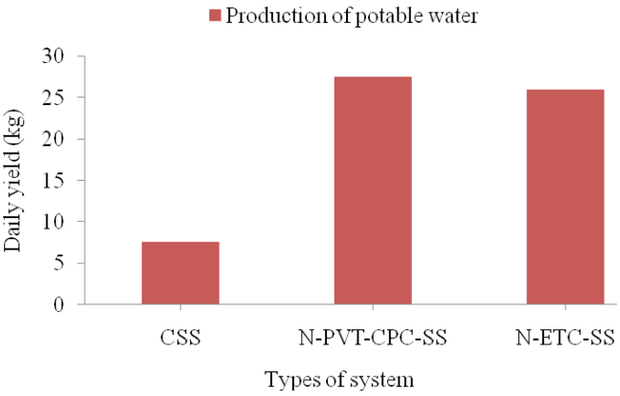

Fig 9. Variation of daily yield with types of system for a typical day in the month of June.

an additional amount of heat is added to basin with the help of *N* identical ETC in the case of N-ETC-SS. However, production of potable water in the case of N-ETC-SS is lower than N-PVT-CPC-SS because of the concentration of beam radiation on the receiver surface after getting reflected from parabolic surface.

Fig. 10 represents the variation of daily exergy gain and daily energy output with types of system at 0.14 m water depth under optimized condition for a typical day in the month of June. It is observed that the value of daily exergy gain in the case of N-ETC-SS is higher by 68.61% than CSS because higher temperature of water is obtained in the case of N-ETC-SS due to the presence of *N* identical collectors. However, exergy gain is lower by 5.47% for N-ETC-SS than N-PVT-CPC-SS. It happens because the optimum value of $\dot{m}_f$ is lower by 150% for N-ETC-SS than N-PVT-CPC-SS. Further, the variation in energy output is similar to the variation in production of potable water because energy output is directly proportional to the production of potable water.

Fig. 11 represents the variation of daily exergy efficiency and daily energy efficiency with types of system at 0.14 m water depth under optimized condition for a typical day in the month of June. It is observed that the daily exergy efficiency is higher by 66.17% for N-ETC-SS than CSS because of their lower input exergy. However, daily exergy efficiency is lower by 0.14% for N-ETC-SS than N-PVT-CPC-SS because the input exergy is lower for N-PVT-CPC-SS. Similarly, the daily energy efficiency is higher by 22.66% and 55.63% for N-ETC-SS than N-PVT-CPC-SS and CSS respectively.

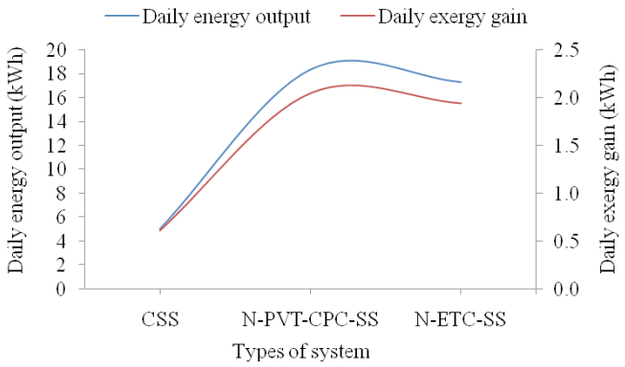

Fig 10. Variation of daily exergy gain and daily energy output with types of system for a typical day in the month of June.

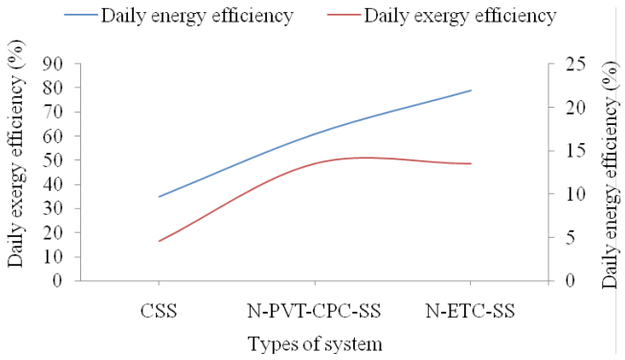

Fig 11. Variation of daily exergy efficiency and daily energy efficiency with types of system for a typical day in the month of June.

6. Conclusions and recommendations

6.1. Conclusions

The thermal modeling and development of characteristics equations have been done for N-ETC-SS. The amount of yield, energy, exergy, exergy efficiency and energy efficiency have been evaluated at 0.14 m water depth under optimized condition for N-ETC-SS for a typical day in the month of June and these results have been compared with results of similar systems reported by various researchers previously. The following conclusions have been drawn on the basis of present research study.

(i) The daily yield is higher by 70.95% and lower by 6.04% for N-ETC-SS than CSS and N-PVT-CPC-SS respectively.
(ii) The daily exergy gain is higher by 68.61%; lower by 5.47% for N-ETC-SS than CSS and N-PVT-CPC-SS

respectively. The variation in energy output is similar to the variation in yield.

(iii) The daily exergy efficiency is higher by 66.17% and lower by 0.14% for N-ETC-SS than CSS and N-PVT-CPC-SS respectively.

(iv) The daily exergy efficiency is higher by 22.66% and 55.63% for N-ETC-SS than N-PVT-CPC-SS and CSS respectively.

6.2. Recommendations

The proposed system should be studied for local climatic condition before its installation. The theoretical results of proposed N-ETC-SS using thermal model developed can be validated by experimental results under optimized condition. The effect of salt concentration/salinity/particulates/nanofluids should be studied.

Symbols

A_b — Area of basin, m²
A_g — Area of glass cover, m²
CPC — Compound parabolic concentrator collector
C — Specific heat capacity, J/kg-K
CSS — Conventional single slope solar still
SS — Single slope solar still
ETC — Evacuated tubular collector
$\dot{E}$ — Hourly energy output, kWh
E — Daily energy output, kWh
FPC — Flat plate collector
F′ — Collector efficiency factor, dimensionless
$\dot{G}_{ex}$ — Hourly exergy gain, kWh
G_{ex} — Daily exergy gain, kWh
h_{cwg} — Convective heat transfer coefficient from water to inner surface of glass cover, W/m²-K
h_{ewg} — Evaporative heat transfer coefficient from water surface to inner surface of glass cover, W/m²-K
h_c — Convective heat transfer coefficient, W/m²-K
h_{ba} — Heat transfer coefficient from blackened surface to ambient, W/m² K
h_{bw} — Heat transfer coefficient from blackened surface to water mass, W/m²-K
h — Heat transfer coefficient, W/m²-K
h_{rwg} — Radiative heat transfer coefficient from water surface to inner surface of glass cover, W/m²-K
h_r — Radiative heat transfer coefficient, W/m²-K
h_{1w} — Total heat transfer coefficient from water surface to inner surface of glass cover, W/m²-K
h_{1g} — Total heat transfer coefficient from water surface to inner glass cover, W/m²-K
$I(t)$ — Solar intensity on collector, W/m²
$I_S(t)$ — Solar intensity on glass cover, W/m²
K — Thermal conductivity, W/m-K
L — Thickness, m
L — Latent heat, J/kg
L' — Length, m
$\dot{m}_f$ — Mass flow rate of fluid/water, kg/s
$\dot{m}_{ew}$ — Mass of distillate from single slope solar still, kg
PF_c — Penalty factor due to the glass covers for the glazed portion
N-ETC-SS — Single slope solar still included with N identical ETC
N-PVT-CPC-SS — Single slope solar still included with N identical CPC
PF_1 — Penalty factor first, dimensionless
PF_2 — Penalty factor second, dimensionless
PVT — Photovoltaic thermal
$\dot{Q}_{uN}$ — Useful energy gain for N identical collector connected in series, kWh
R_{o1} — Inner radius of outer glass tube of evacuated coaxial glass tube, m
R_{i2} — Outer radius of inner glass tube of evacuated coaxial glass tube, m
R_{o2} — Outer radius of outer glass tube of evacuated coaxial glass tube, m
r' — Radius of copper tube in ETC
R' — Reflectivity
T_{foN} — Outlet water temperature at the end of Nth water collector, °C
T_{fi} — Water temperature at the inlet of 1st ETC, °C
T_a — Ambient temperature, °C
T_{gi} — Glass temperature at inner surface of glass cover, °C
t — Time, h
T_{wo} — Water temperature at t=0, °C
T_w — Water temperature, °C
U_L — Overall heat transfer coefficient
V — Velocity of air, m/s

Subscript

b — Basin liner
eff — Effective
en — Energy
ex — Exergy
f — Fluid
g — Glass
in — Incoming
out — Outgoing
w — Water

Greek letters

α — Absorptivity (fraction)
η — Efficiency, %
$(\alpha\tau)_{eff}$ — Product of effective absorptivity and transmittivity
σ — Stefan–Boltzmann constant, W/m²-K⁴
η_{cN} — Temperature dependent electrical efficiency of solar cells of a number

(N) of PVT-FPC/CPC water collectors

τ — Transmittivity

References

[1] S.N. Rai, G.N. Tiwari, Single basin solar still coupled with flat plate collector, Energy Convers. Manage., 23(3) (1983) 145–149.

[2] G.M. Zaki, T. El Dali, H. ElShafie, Improved performance of solar still, Proc. First Arab Int. Solar Energy Conf., Kuwait, (1983) 331–335.

[3] Y.P. Yadav, S.K. Yadav, Parametric studies on the transient performance of a high temperature solar distillation system, Desalination, 170 (2004) 251–262.

[4] O.O. Badran, H.A. Al-Tahaineh, The effect of coupling flat plate collector on the solar still productivity, Desalination, 183 (2004) 137–142.

[5] Z.S. Abdel-Rehim, A. Lasheen, Experimental and theoretical study of a solar desalination system located in Cairo, Egypt, Desalination, 217 (2007) 52–64.

[6] R. Tripathi, G.N. Tiwari, Effect of water depth on internal heat and mass transfer for active solar distillation, Desalination, 173 (2005) 187–200.

[7] A.A. Badran, A.A. Al-Hallaq, I.A.E. Salman, M.Z. Odat, A solar still augmented with a flat-plate collector, Desalination, 172 (2005) 227–234.

[8] H. Taghvaei, H. Taghvaei, M.R. KhosrowJafarpur, M. Karimi Estahbanati, A.M. Feilizadeh, A. Seddigh, A thorough investigation of the effects of water depth on the performance of active solar stills, Desalination, 347 (2014) 77–85.

[9] A.A. El-Sebaii, S.J. Yaghmour, F.S. Al-Hazmi, A.S. Faidah, F.M. Al-Marzouki, A.A. Al-Ghamdi, Active single basin solar still with a sensible storage medium, Desalination, 249 (2009) 699–706.

[10] M. Arslan, Experimental investigation of still performance for different active solar still designs under closed cycle mode, Desalination, 307 (2012) 9–19.

[11] M. Lilian, M.A. George, M. Al-Hindi, The effect of cover geometry on the productivity of a modified solar still, Desalination unit, Energy Procedia, 50 (2014) 406 – 413.

[12] T. Rajaseenivasana, P. Nelson, K. Srithar, An experimental investigation on a solar still with an integrated flat plate collector, Desalination, 347 (2014) 131–137.

[13] O.A. Hamadou, K. Abdellatif, Modeling an active solar still for sea water desalination process optimization, Desalination, 354 (2014) 1–8.

[14] F. Calise, M.D. d'Accadia, A. Piacentino, A novel solar trigeneration system integrating PVT (photovoltaic/thermal collectors) and SW (seawater) desalination: Dynamic simulation and economic assessment, Energy, 67 (2014) 129–148.

[15] A.G.M. Ibrahim, E.E. Allam, S.E. Elshamarka, A modified basin type solar still: Experimental performance and economic study, Energy, 93 (2015) 335–342.

[16] E.C. Kern, M.C. Russell, Combined photovoltaic and thermal hybrid collector systems, In: Proceedings of the 13th IEEE Photovoltaic Specialists, June 5–8. Washington, DC, USA, (1978) 1153–1157.

[17] S.D. Hendrie, Evaluation of combined photovoltaic/thermal collectors, In: Proceedings of international conference ISES, vol. 3. Atlanta, GA, USA, (1979) 1865–1869.

[18] S. Kumar, A. Tiwari, An experimental study of hybrid photovoltaic thermal (PV/T) active solar still, Int. J. Energy Res., 32 (2008) 847–58.

[19] S. Kumar, G.N. Tiwari, Estimation of internal heat transfer coefficients of a hybrid (PV/T) active solar still, Solar Energy, 83 (2009) 1656–1667.

[20] S. Kumar, G.N. Tiwari, Life cycle cost analysis of single slope hybrid (PV/T) active solar still, Appl. Energy, 86 (2009a) 1995–2004.

[21] S. Kumar, A. Tiwari, Design, fabrication and performance of a hybrid photovoltaic/thermal (PVT)active solar still, Energy Convers. Manage., 51 (2010) 1219–1229.

[22] S. Kumar, G.N. Tiwari, M.K. Gaur, Development of empirical relation to evaluate the heat transfer coefficients and fractional energy in basin type hybrid (PVT) active solar still, Desalination, 250 (2010a) 214–221.

[23] G. Singh, S. Kumar, G.N. Tiwari, Design, fabrication and performance of a hybrid photovoltaic/thermal (PVT) double slope active solar still, Desalination, 277 (2011) 399–406.

[24] G.N. Tiwari, J.K. Yadav, D.B. Singh, I.M. Al-Helal, A.M. Abdel-Ghany, Exergoeconomic and enviroeconomic analyses of partially covered photovoltaic flat plate collector active solar distillation system, Desalination, 367 (2015) 186–196.

[25] D.B. Singh, J.K. Yadav, V.K. Dwivedi, S. Kumar, G.N. Tiwari, I.M. Al-Helal, Experimental studies of active solar still integrated with two hybrid PVT collectors, Solar Energy, 130 (2016) 207–223.

[26] M.K. Gaur, G.N. Tiwari, Optimization of number of collectors for integrated PV/T hybrid active solar still, Appl. Energy, 87 (2010) 1763–1772.

[27] M.A. Eltawil, Z.M. Omara, Enhancing the solar still performance using solar photovoltaic flat plate collector and hot air, Desalination, 349 (2014) 1–9.

[28] F. Saeedi, F. Sarhaddi, A. Behzadmehr, Optimization of a PV/T (photovoltaic/thermal) active solar still, Energy, 87 (2015) 142–152.

[29] D.B. Singh, G.N. Tiwari, Effect of energy matrices on life cycle cost analysis of partially covered photovoltaic compound parabolic concentrator collector active solar distillation system, Desalination, 397 (2016) 75–91.

[30] D.B. Singh, G.N. Tiwari, Performance analysis of basin type solar stills integrated with N identical photovoltaic thermal (PVT) compound parabolic concentrator (CPC) collectors: A comparative study, Solar Energy, 142 (2017) 144–158.

[31] D.B. Singh, G.N. Tiwari, Exergoeconomic, enviroeconomic and productivity analyses of basin type solar stills by incorporating N identical PVT compound parabolic concentrator collectors: A comparative study, Energy Convers. Manage., 135 (2017) 129–147.

[32] R.V. Singh, S. Kumar, M.M. Hasan, M.E. Khan, G.N. Tiwari, Performance of a solar still integrated with evacuated tube collector in natural mode, Desalination, 318 (2013) 25–33.

[33] S. Kumar, A. Dubey, G.N. Tiwari, A solar still augmented with an evacuated tube collector in forced mode, Desalination, 347 (2014) 15–24.

[34] D.B. Singh, G.N. Tiwari, I.M. Al-Helal, V.K. Dwivedi, J.K. Yadav, Effect of energy matrices on life cycle cost analysis of passive solar stills, Solar Energy, 134 (2016) 9–22.

[35] R.K. Mishra, V. Garg, G.N. Tiwari, Thermal modeling and development of characteristic equations of evacuated tubular collector (ETC), Solar Energy, 116 (2015) 165–176.

[36] J. Fernandez, N. Chargoy, Multistage indirectly heated solar still, Solar Energy, 44(4) (1990) 215.

[37] S. Toyama, K. Kagakuv, Gijitsu, 24, (1972) 159, Maruzen, Tokyo.

[38] P.K. Nag, Basic and applied thermodynamics, Tata McGraw-Hill, 2004.

[39] G.N. Tiwari, Solar Energy, fundamentals, design, modeling and application, Narosa Publishing House, New Delhi, 2013.

[40] R. Tripathi, G.N. Tiwari, I.M. Al-Helal, Thermal modeling of N partially covered photovoltaic thermal (PVT) – Compound parabolic concentrator (CPC) collectors connected in series, Solar Energy, 123 (2016) 174–184.

Appendix-A

Expressions for a_1 and $f_1(t)$ used in Eq. (7) and expressions of heat transfer coefficients used in Eqs. (9) to (11) are as follows.

$$a_1 = \frac{1}{M_w C_w}\left[\dot{m}_f C_f \left(1 - K_k^N\right) + U_s A_b\right]$$

$$f_1(t) = \frac{1}{M_w C_w}\left[\alpha'_{eff}\ A_b I_s(t) + \frac{\left(1 - K_k{}^N\right)}{\left(1 - K_k\right)}(AF_R(\alpha\tau))_1 I_b(t) + \left(\frac{\left(1 - K_k{}^N\right)}{\left(1 - K_k\right)}\left(AF_R U_L\right)_1 + U_s A_b\right)T_a\right];$$

$$\alpha'_{eff} = \alpha'_w + h_1\alpha'_b + h'_1\alpha'_g$$

$$h_1 = \frac{h_{bw}}{h_{bw} + h_{ba}}; h'_1 = \frac{h_{1w}A_g}{U_{c,ga}A_g + h_{1w}A_b}; h_{1w} = h_{rwg} + h_{cwg} + h_{ewg};$$

$$h_{e,wg} = 16.273 \times 10^{-3} h_{c,wg}\left[\frac{P_w - P_{gi}}{T_w - T_{gi}}\right];$$

$$h_{c,wg} = 0.884\left[\left(T_w - T_{gi}\right) + \frac{\left(P_w - P_{gi}\right)\left(T_w + 273\right)}{268.9 \times 10^3 - P_w}\right]^{\frac{1}{3}};$$

$$P_w = \exp\left[25.317 - \frac{5144}{T_w + 273}\right];$$

$$P_{gi} = \exp\left[25.317 - \frac{5144}{T_{gi} + 273}\right];$$

$$h_{rwg} = \left(0.82 \times 5.67 \times 10^{-8}\right)\left[(T_w + 273)^2 + (T_{gi} + 273)^2\right]\left[T_w + T_{gi} + 546\right]$$

$$U_s = U_t + U_b; U_b = \frac{h_{ba}h_{bw}}{h_{bw} + h_{ba}}; U_t = \frac{h_{1w}U_{c,ga}A_g}{U_{c,ga}A_g + h_{1w}A_b};$$

$$U_{c,ga} = \frac{\frac{K_g}{l_g}h_{1g}}{\frac{K_g}{l_g} + h_{1g}}; h_{ba} = \left[\frac{L_i}{K_i} + \frac{1}{h_{cb} + h_{rb}}\right]^{-1};$$

$$h_{cb} + h_{rb} = 5.7 W m^{-2} K^{-1}, h_{bw} = 100 W m^{-2} K^{-1};$$